JOINT INSTITUTE FOR NUCLEAR RESEARCH
Bogoliubov Laboratory of Theoretical Physics (BLTP)

FINAL REPORT ON THE INTEREST PROGRAMME

Numerical simulations for the IV-characteristics for Josephson junctions

Supervisor:
Dr. Majed Nashaat
BLTP, JINR, Dubna, Russia

Student:
Rawda Hafez, Egypt
Cairo University

Participation period:
November 05 – December 14,
Wave 11

Dubna, 2024

Abstract

During this practice, we study the current-voltage characteristics (IV) of superconducting-insulator-superconductor (SIS) Josephson Junctions under various conditions. Initially, we examined it in the frame of resistively and capacitively shunted junction model, highlighting the influence of the Stewart-McCumber parameter (β). We demonstrate also the influence of external radiation and the presence of the Shapiro steps on the I-V curve.

Furthermore, we explored a coupled system of a Josephson Junction and a nanomagnet. In this system, we combine the RCSJ model with the Landau-Lifshitz-Gilbert (LLG) equation. Here, we demonstrate the reorientation of the nanomagnet's easy axis. These findings provide insights into the interplay between Josephson Junction dynamics and nanomagnetic coupling, contributing to a deeper understanding of such hybrid systems.

Introduction

Six decades ago, in 1962, Brian Josephson made a revolutionary prediction centered around what is now known as the Josephson effect. At the heart of this effect lies the Josephson junction (JJ). The Josephson junction is a fundamental electronic device, making it a cornerstone of modern superconducting technology. It comprises two superconductors separated by thin barriers, forming a weak link. This barrier could be an insulating material (SIS), ferromagnetic material (SFS), etc. The operation of the Josephson junction is governed by quantum tunneling, where Cooper pairs (pairs of electrons with opposite spins and momenta) can tunnel through the barrier from one superconductor to the other with zero resistance. However, there are two modes of pair tunneling: DC and AC Josephson effect, which can be described using Josephson equations.

1.1 Josephson equations

1.1.1 Josephson 1st equation

When Cooper pairs (supercurrent) flow through a Josephson junction in the absence of an applied voltage $V = 0$, the current of this supercurrent will be given as:

$$I_s = I_c \sin(\Delta\varphi), \qquad (1)$$

where:

I_s: The supercurrent across the junction.

I_c: the critical current, the maximum supercurrent the junction can carry without breaking superconductivity.

$\Delta\varphi = \varphi_1 - \varphi_2$: The phase difference between the superconducting wavefunctions on either side of the junction.

This shows that the flow current depends only on the phase difference between the superconducting wavefunctions. $\Psi_1 = |\Psi_1| e^{i\varphi_1}$ $\Psi_2 = |\Psi_2| e^{i\varphi_2}$ on either side of the junction. Eq. (1) directly defines the DC Josephson effect. It shows that the supercurrent is not proportional to voltage (as in Ohm's law) but depends on the quantum mechanical phase difference.

1.1.2 Josephson 2nd Equation

The second Josephson equation is central to understanding the AC Josephson effect, which describes the supercurrent's oscillatory behavior when a constant voltage ($V \neq 0$) is applied across Josephson Junction and is given by:

$$\frac{d\Delta\varphi}{dt} = \frac{2eV}{\hbar} \qquad (2)$$

Eq. (2) expresses how the phase difference between the superconducting wavefunctions evolves over time in response to an applied voltage, where the rate of phase evolution is directly proportional to the voltage. The phase difference as a function of time can be derived as $\Delta\varphi(t) = \Delta\varphi_0 + \frac{2eV}{\hbar}t$.

Thus, the current will become time-dependent. $I_s(\mathrm{t}) = I_c \sin\left(\Delta\varphi_0 + \frac{2eV}{\hbar}t\right)$ will oscillate with an angular frequency ω_J where:

$$\omega_J = \frac{2eV}{\hbar} \qquad (3)$$

This is known as Josephson frequency.

1.2 Single Junction

Josephson junctions can be constructed in various ways, depending on the material used for the barrier and the number of junctions involved. Our concern here is the superconductor-insulator-superconductor (SIS) single junction. This represents the simplest form of a Josephson device, consisting of two superconducting electrodes separated by a thin layer of an insulating barrier, forming a weakly superconducting. This structure is the basic unit for investigating the Josephson effect and is the foundation for more complex superconducting circuits.

1.2.1 Resistively and Capacitively Shunted Junction Model

The resistively and capacitively shunted junction (RCSJ) model is a widely used equivalent circuit model for understanding the behavior of a single Josephson junction. This effectively captures the junction's dynamics in the presence of both superconducting and normal currents.

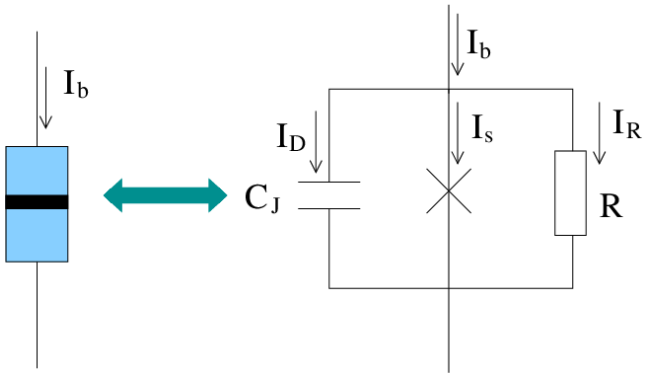

Figure 1: Circuit diagram of the RCSJ model for a current-biased JJ (Rengifo, 2008).

Fig (1) represents the junction as a combination of three parallel components: a resistor (R), a capacitor (C_J), and an ideal Josephson element:

Resistor (R):

Represents the normal current flowing through the junction when it is in the resistive state. Models the dissipative losses due to quasiparticle tunneling. Governed by Ohm's law $I_R = I_{qp} = \frac{V}{R}$, where I_{qp} stands for the current of quasiparticles.

Capacitor (C):

Represents the capacitance due to the junction's physical structure, particularly the insulating barrier. It captures the junction's ability to store charge and causes inertial effects in the phase dynamics. Governed by $I_C = I_{disp} = C\frac{dV}{dt}$ where I_{disp} stands for displacement current.

Ideal Josephson Element:

Represents the superconducting current due to Cooper pair tunneling. Governed by the first Josephson equation: $I_s = I_c \sin(\Delta\varphi)$

Thus, the total current through the Josephson junction is the sum of the contributions from the three components:

$$I = I_{qp} + I_{disp} + I_S \qquad (4)$$

Substituting the expressions for each component:

$$I = \frac{V}{R} + C\,\frac{dV}{dt} + I_c \sin(\Delta\varphi) \qquad (5)$$

1.2.2 Establishing the model

Our main goal is to examine the phase dynamics of the single JJ, which can be solved numerically using the Runge-Kutta method. This can be done using C++. However, we must first normalize Eq. (2) and Eq. (5) using the following parameters to perform the calculations:

$$V_0 = \frac{\hbar\omega_P}{2e}$$

$$\tau = \omega_P \text{ where } \omega_P = \sqrt{\frac{2eI_c}{C\hbar}}$$

$$\beta = \frac{1}{R}\sqrt{\frac{\hbar}{2eI_cC}}$$

Where $\frac{I}{I_c} \to I$ and $\frac{V}{V_o} \to V$

Thus, we can rewrite Eq. (2) and Eq. (5) as follows:

$$\frac{\partial\varphi}{\partial t} = V$$

$$I = \beta\frac{\partial\varphi}{\partial t} + \frac{dV}{dt} + \sin(\varphi)$$

1.2.3 Results and Conclusion

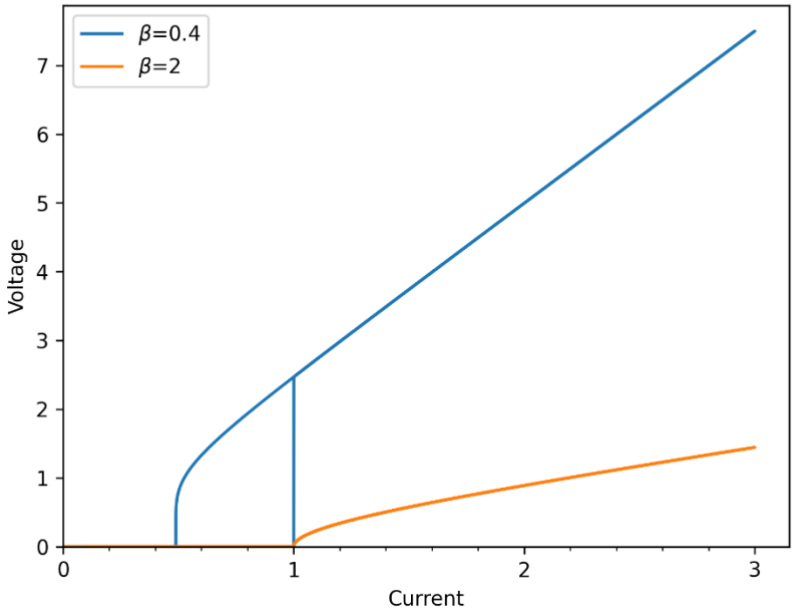

Figure 2: The current-voltage characteristics (IV) plot for different values of β.

As shown in Fig (2), each graph can be represented in two regions:

Superconducting state:
The current that flows through the junction is below the critical current ($I < I_c$), which we call the supercurrent (cooper pairs). This current flows without resistance, exhibiting zero voltage across the junction. This is due to the coherent tunneling of Cooper pairs, which do not experience dissipation.

Resistive state:
A voltage across the junction appears when the current exceeds the critical current value ($I > I_c$). The quasiparticles flow as a dominant current following the ohmic voltage relation., where the resistance in this region will not be equal to zero.

We can categorize the junction's damping behavior as overdamped or underdamped based on the dimensionless parameter. β, the Stewart-McCumber parameter, which is given as:

$$\beta = \frac{1}{R}\sqrt{\frac{\hbar}{2eI_cC}}$$

Underdamped Regime (β <1):
The current in the junction exhibits oscillatory behavior due to the dominance of the junction's capacitance over the resistance. However, in the reverse, when the current is reduced below I_c , the voltage does not immediately drop to zero again. The junction stays in the resistive state until the current falls significantly lower than I_c. This forms a hysteresis loop, the size of which depends on β's value. This is demonstrated in Fig (2) where β = 0.2.

Overdamped Regime (β >1):
There is no oscillatory behavior of the phase difference across the junction, so the current transitions smoothly between states without oscillations due to high energy dissipation through the resistor. The capacitance has a negligible effect on the dynamics, and no hysteresis is observed in the I-V curve. This is demonstrated in Fig (2) where β = 4.

1.3 Effects of External Radiation

When a Josephson junction is exposed to external AC radiation (electromagnetic field), a unique phenomenon emerges due to the interaction of the external radiation with the superconducting current, which is the appearance of Shapiro steps**.** The cause of Shapiro's steps lies in the interaction between the external AC radiation and the intrinsic Josephson oscillations. This interaction leads to phase-locking of the junction oscillation by this n^{th} harmonic, which generates discrete voltage plateaus in the junction's current-voltage I-V characteristics. In order to see Shapiro's steps in the IV curve, we introduce an external AC current source to Eq (5) by $I_{ac}sin\ (\Omega t)$, where I_{ac} and Ω are the amplitude and the frequency of the external source.

In Fig. (3), we demonstrate our simulations at different values of dissipation at A=2 (where A is the normalized amplitude of the external AC source, A= I_{ac}/ I_c), and ω=0.5 (normalized frequency of the external drive).

As shown in Fig (3), the position of Shapiro steps depends as well on the value of β , where:

At β = 4, in overdamped regime. Shapiro's steps are well-defined and regular, and they appear only on integer values of the angular frequency (plasma frequency) multiples

and are equal to the normalized time-averaged voltage. $V_n = n\omega$, since $\omega = 0.5$ it appears that the first and the second harmonics are located at $V = 0.5$ and $V = 1$.

At β = 0.2, in underdamped regime. In addition to the integer Shapiro steps, we have steps at fractional values of ω as shown in Fig (3). However, there is no presence of the Hysteresis loop.

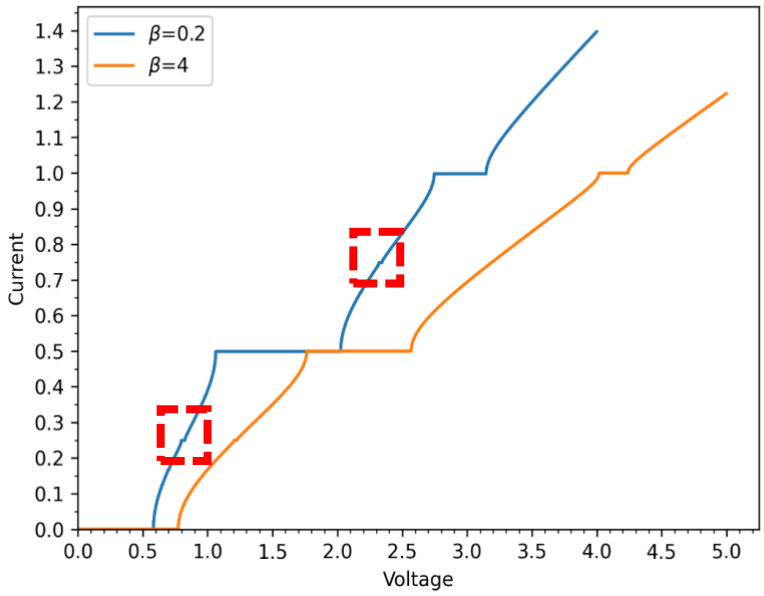

Figure 3: The current-voltage characteristics of different values of β

2. Interaction of a nanomagnet with a weak superconducting link

In this section, we highlight a study of an electromagnetic hybrid system that consists of a nanomagnet that interacts with a Josephson junction through magnetic fields. Such systems combine superconducting and magnetic phenomena, offering a rich interplay of spin dynamics and superconductivity.

2.1 Coupling Mechanism

In this setup, a nanomagnet is located close to the weak link between two superconductors but away from the path of the tunneling current. So, the interaction between the two systems is considered purely electromagnetic. The magnetic field of the nanomagnet, which originates from its magnetic dipole moment (M), influences the Josephson current flowing through the link (I_s) and induces changes in the phase difference (φ). This alternation generates an oscillating magnetic flux in the Josephson junction that acts back on the nanomagnet, affecting spin dynamics. However, the final magnetic field that affects the magnetic moment is called the effective field and is given by:

$$\boldsymbol{H}_{eff} = \boldsymbol{H}_o - \frac{\partial K(M)}{\partial \boldsymbol{M}} + \boldsymbol{H}_J \qquad (2.1)$$

Where:

$\boldsymbol{H}_o$: an external applied magnetic field

K(M): The anisotropy energy, the energy barrier that stabilizes the magnetization along its easy axis

- $\frac{\partial K(M)}{\partial \boldsymbol{M}}$: The Magnetic Anisotropy

$\boldsymbol{H}_J$**:** The magnetic field generated by the oscillating Josephson current

The dynamic coupling between the nanomagnet and the weak superconducting link will cause the magnetic moments to rotate around the effective magnetic field (H_{eff}), driven by a torque that can be described as:

$$\frac{d\boldsymbol{M}}{dt} = -\gamma \boldsymbol{M}\, x \boldsymbol{H_{eff}} \qquad (2.2)$$

Where:

γ: The gyromagnetic ratio of the angular momentum to the magnetic moment. The -ve sign determines the direction of precession (opposite to the torque direction)

Eq. (2.2) is an equation of motion that shows the spiral-like motion of the magnetic moment, called the precessional motion. However, this equation is considered a description of an idealized case of motion. In real systems, energy experiences dissipation. To account for this, we include the damping term, leading to:

$$\frac{d\boldsymbol{M}}{dt} = -\gamma \boldsymbol{M}\, x\, \boldsymbol{H_{eff}} + \frac{\alpha}{M_s} \boldsymbol{M}\, x\, \frac{d\boldsymbol{M}}{dt} \qquad (2.3)$$

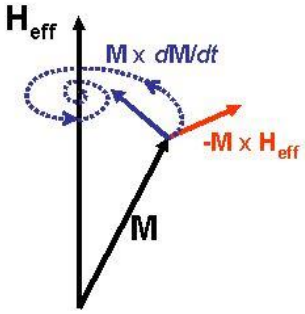

Where α is the Gilbert damping constant, and M_s is the saturation magnetization. However, this damping term ensures that the magnetic moment eventually aligns with ($\boldsymbol{H_{eff}}$). This equation is called the **Landau-Lifshitz-Gilbert (LLG) Equation**, which represents the nonlinear dynamics of this coupled system. Landau and Lifshitz proposed it in 1935, and Gilbert successively modified the damping term in 1955.

2.2 Establishing the model

To investigate the dynamical model of JJ-coupled nanomagnet, we can numerically solve the LLG equation using the Gause-Legendre method. So, we need to turn the quantities into dimensionless quantities.
Thus, the magnetic moment component in the LLG equation is given by:

$$\frac{dm}{d\tau} = -\frac{\Omega_0}{(1 + M^2\alpha^2)}\left(m \times h_{eff} + \alpha\left[m \times \left(m \times h_{eff}\right)\right]\right)$$

In 3D

$$\frac{dm_z}{d\tau} = \frac{\Omega_F}{(1+\alpha^2)}\left[\alpha\tilde{h}_z\left(m_x^2+m_y^2\right) - h_y\left(m_x+\alpha m_y m_z\right) + h_x\left(m_y-\alpha m_x m_z\right)\right]/D$$
$$\frac{dm_x}{d\tau} = \frac{\Omega_F}{(1+\alpha^2)}\left[h_y\left(m_z-\alpha m_x m_y\right) - h_z\left(\alpha m_x m_z+m_y\right) + \alpha h_x\left(m_y^2+m_z^2\right)\right]$$
$$\frac{dm_y}{d\tau} = \frac{\Omega_F}{(1+\alpha^2)}\left[-h_x\left(\alpha m_x m_y+m_z\right) + h_z\left(m_x-\alpha m_y m_z\right) + \alpha h_y\left(m_x^2+m_z^2\right)\right]$$

Where:

$$D = 1 + \frac{\Omega_0\alpha\epsilon k}{1+M^2\alpha^2}\left(m_x^2+m_y^2\right)$$

The effective field components are:

$$\begin{aligned} h_x &= 0 \\ h_y &= m_y \\ \tilde{h}_z &= \epsilon\left(\sin\left(\omega_j t - k m_z\right) + \omega_j + k\dot{m}_z\right) \\ h_z &= \tilde{h}_z - \epsilon k\dot{m}_z \end{aligned}$$

Where $\epsilon = Gk$.

2.3 Results and Conclusion

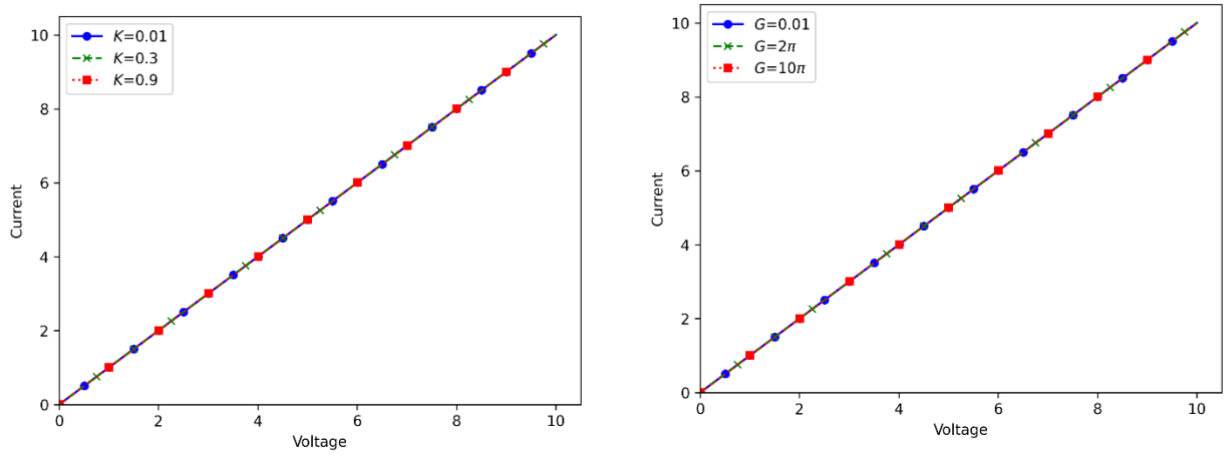

Figure 4: The current-voltage characteristics (IV) plot for different values of K and G.

As shown in Fig (4), the IV Characteristic isn't sensitive to system dynamics as it's the same whenever you change the value of the initial parameters. So, in order to investigate the dynamics of this coupled system, we need to consider the orientation of the magnetic moments.

2.3.1 Reorientation of an easy-axis

- $k = 0.01 \; and \; G = \pi$

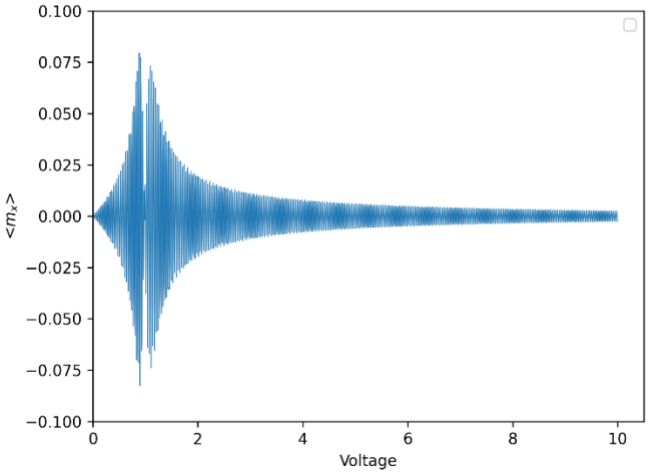

Figure a

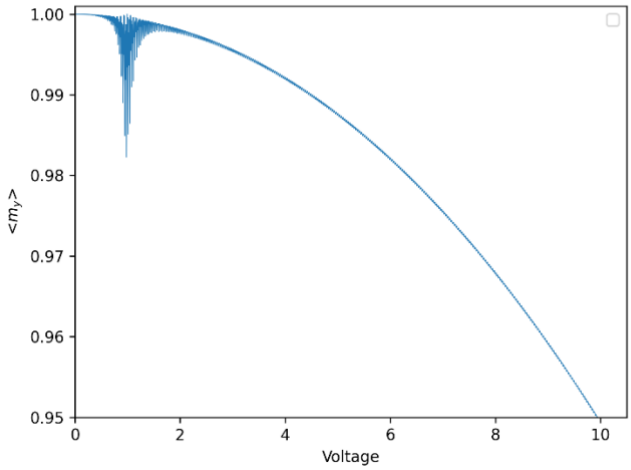

Figure b

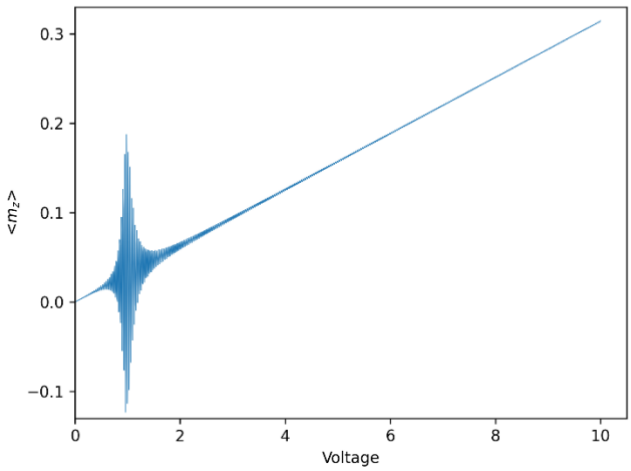

Figure c

Figure 5: shows the orientation of magnetic moments in each direction

Fig (5) shows that, initially, the direction of the magnetic moments is on the y-axis $<m_y> = 1$. Due to the coupling with the JJ and by increasing the voltage gradually, the magnetic moments start to reorient from its initial easy axis. However, due to the small

value of k = 0.01, the magnetic moment will not experience a complete reorientation; this can be seen through $< m_x >$ and $< m_y >$ that they didn't reach zero value. And $< m_z >$ didn't reach 1 as well. Now, at strong coupling (see Fig (6)), a complete reorientation at V=2 can be achieved where $< m_x >$ started from zero and ended at zero, and $< m_y >$ starts from one and ended at zero, while $< m_z >$starts from 0 and end at 1, which indicates the complete reorientation of the easy axis.

- $k = 0.3\ and\ G = \pi$

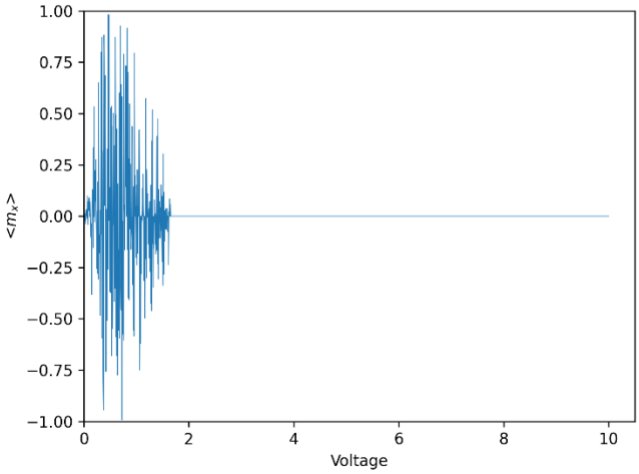

Figure a

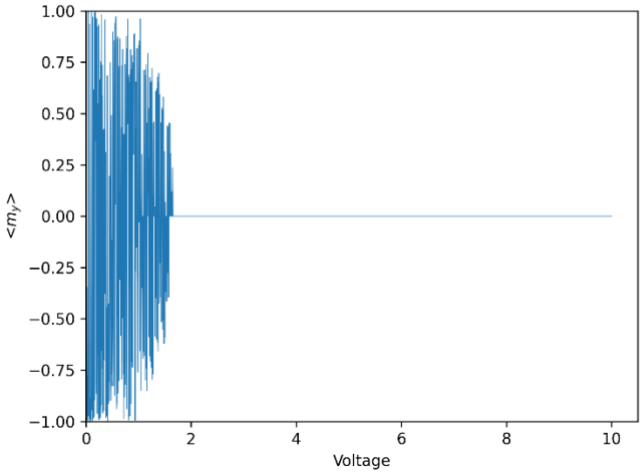

Figure b

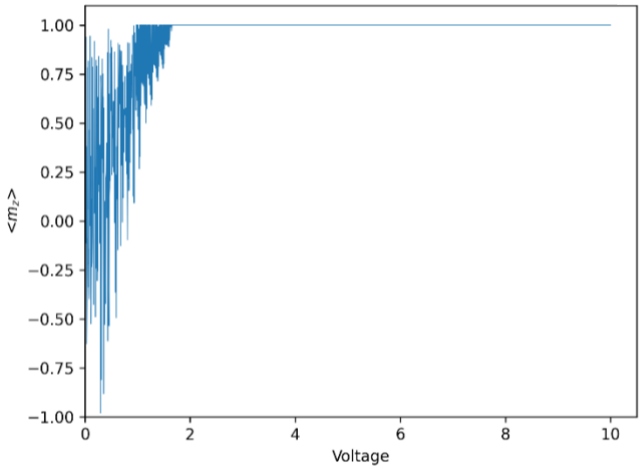

Figure c

Figure 6: shows the orientation of magnetic moments in each direction.

3. Conclusion

In the study, we examined the current-voltage characteristics of Josephson Junction under different conditions. We began with an SIS Josephson Junction within the RCSJ circuit and saw how alternating the value of the Stewart-McCumber parameter (β) can affect the shape of the IV- characteristics. The value β changes with changing the capacitance and resistance values, affecting the oscillatory behavior of the current. Thus, we can categorize the IV- characteristics based on whether they are underdamped or overdamped.

We applied the same approach when introducing an external radiation source. By examining the phase-locking phenomenon, we explored the origin of the discrete voltage plateaus that appear on the IV- characteristics, known as Shapiro's steps. This is due to the interaction between the external radiation and the AC Josephson effect. This interaction causes the junction's oscillations to synchronize with the radiation frequency, resulting in phase-locked steps on the voltage.

Additionally, we studied the Josephson Junction nanomagnet coupled system. By checking the IV- characteristics for the coupling model at different parameters using Landau-Lifshitz-Gilbert (LLG), we can deduce that the IV- characteristics cannot detect the dynamics that happened in the system. However, by checking the values of the magnetic moments in each direction, we can understand the effect that had happened on the nanomagnet as a result of the coupling mechanism, which can be described as the reorientation of the magnetic moments for the easy axis to the direction of the effective field due to Josephson energy.

Acknowledgments

I would like to express my sincere gratitude to Dr. Majed Nashaat for his extraordinary patience and invaluable guidance throughout the practice. I am truly grateful for the opportunity to work with him and the enriching experience that has significantly contributed to my personal and academic growth.

I would also like to thank JINR interest for providing students with the opportunity to engage in research, offering us the chance to deepen our understanding of the scientific process, and expanding our knowledge in advanced topics.

Lastly, I extend my thanks to Prof. Yu M. Shukrinov and his research group for generously sharing their work with us.

References

d'Aquino, M.
Nonlinear Magnetization Dynamics in Thin-films and Nanoparticles. (2004).

K. V. Kulikov, D. V. Anghel, M. Nashaat, M. Dolineanu, M. Sameh, and Yu. M. Shukrinov.
Resonance phenomena in a nanomagnet coupled to a Josephson junction under external periodic drive. *Phys. Rev. B* ***109****, 014429 (2024).*

L. Cai and E. M. Chudnovsky.
Interaction of a nanomagnet with a weak superconducting link. *Phys. Rev. B* ***82****, 104429 (2010).*

Ramón Aguado, R. C.
New Trends and Platforms for Quantum Technologies. Springer.(2024)

Rengifo, R.
Quantum breathers in small networks: Dynamics, tunneling, correlations, and application to Josephson cells (2008).

RuslanProzorov, C. P.
Superconductivity. ELSEVIER (2007).